Transient Valence Charge Localization in Strong-Field Dissociative Ionization of HCl Molecules

Junyang Ma,[1,2] Liang Xu,[3,4] Hongcheng Ni,[1,5,*] Chenxu Lu,[1] Wenbin Zhang,[1] Peifen Lu,[1] Jin Wen,[6] Feng He,[3,7] Olivier Faucher,[2] and Jian Wu[1,5,7,†]

[1]*State Key Laboratory of Precision Spectroscopy, East China Normal University, Shanghai 200241, China*
[2]*Laboratoire Interdisciplinaire CARNOT de Bourgogne, UMR 6303 CNRS-Université Bourgogne Franche-Comté, BP 47870, 21078 Dijon, France*
[3]*Key Laboratory for Laser Plasmas (Ministry of Education) and School of Physics and Astronomy, Collaborative Innovation Center for IFSA (CICIFSA), Shanghai Jiao Tong University, Shanghai 200240, China*
[4]*Shanghai Key Lab of Modern Optical System, University of Shanghai for Science and Technology, Shanghai 200093, China*
[5]*Collaborative Innovation Center of Extreme Optics, Shanxi University, Taiyuan, Shanxi 030006, China*
[6]*State Key Laboratory for Modification of Chemical Fibers and Polymer Materials and College of Materials Science and Engineering, Donghua University, Shanghai 201620, China*
[7]*CAS Center for Excellence in Ultra-intense Laser Science, Shanghai 201800, China*

(Received 21 October 2020; revised 6 September 2021; accepted 27 September 2021; published 26 October 2021)

Probing transient charge localization in the innershell orbital of atoms and molecules has been made possible by the recent progress of advanced light sources. Here, we demonstrate that the ultrafast electron tunneling ionization by an intense femtosecond laser pulse could induce an asymmetric transient charge localization in the valence shell of the HCl molecule during the dissociative ionization process. The transient charge localization is encoded in the laser impulse acquired by the outgoing ionic fragments, and the asymmetry is revealed by carefully examining the electron tunneling-site distinguished momentum angular distribution of the ejected H^+ fragments. Our work proposes a way to visualize the transient valence charge motion and will stimulate further investigations of the tunneling-site-sensitive ultrafast dynamics of molecules in strong laser fields.

DOI: 10.1103/PhysRevLett.127.183201

In the molecular bonding theory, the valence electrons are delocalized among the composing atoms, providing the bond thereby stabilizing the system. The innershell electrons of individual atoms are, on the other hand, tightly bound to the atoms themselves, which are therefore considered localized. With recent progress in advanced light sources, such as the synchrotron radiation and x-ray free-electron laser, probing innershell electron holes of an atom or molecule becomes accessible [1–7]. This prospect, made possible by the photonic (energy) characteristics of the stimulating field, has led to profound discoveries in the properties of the transient core vacancy left after the removal of innershell electrons, such as the localization and delocalization of K-shell electrons in the van der Waals dimers [8] and creation of double core holes [9–12]. Conversely, one may postulate that the optical (field) characteristics of an intense femtosecond laser pulse could also lead to an electron hole localization [13], especially in the valence molecular shell, when the strength of the oscillating electric field is comparable to the binding of the valence electron thereby breaking the static balance of charge distribution in the molecule [14]. The transient electron localization has been studied theoretically [15–18], which has been shown to lead to multiple ionization bursts within half-laser cycles [17–19] and alter the emission time and initial velocity of the electron [20]. However, the transient charge (or electron hole) localization upon electron tunneling by an intense femtosecond laser field from a valence molecular shell, which is itself primarily delocalized and establishes the molecular bonding, has not been directly observed so far due to its complicated nature and the associated difficulty in singling out its effect to the system.

In this Letter, we uncover the strong-field electron tunneling ionization induced asymmetric transient valence charge localization by tracking the laser impulse acquired by the outgoing ionic fragments during the dissociative single ionization of a diatomic molecule. In this process, the center of mass of the ejected electron and nuclear fragments stays at rest (neglecting photon linear momentum [21,22]) ensured by the neutral state of the parent molecule. While the electron is released from the target, the produced ion experiences a field-induced momentum shift via accumulating the impulse from the laser field

$$\boldsymbol{p}_{\mathrm{ion}} = \int Z_{\mathrm{ion}}(t)\boldsymbol{E}(t)\,dt, \tag{1}$$

 © 2021 American Physical Society

where the transient ionic charge $Z_{\mathrm{ion}}(t)$ naturally sets in, with its effect enlarged by the coupling to the laser electric field $\boldsymbol{E}(t)$ and manifested in the asymptotic momentum $\boldsymbol{p}_{\mathrm{ion}}$ of the ion.

The HCl molecule is taken as a target to explore the asymmetrical transient valence charge localization stimulated by an intense elliptically polarized near-infrared femtosecond laser pulse. In the dissociative single ionization of HCl, the electron is removed from the next highest occupied molecular orbital (HOMO-1) [23] and HOMO-2, which are both σ orbitals. Electron removal from the HOMO does not lead to dissociation [23] and this channel is thus not considered in our study. The electron may tunnel out along the bond direction with a tunneling exit near either the H or Cl site. An asymmetry in the asymptotic H^+ momentum is observed by identifying the tunneling site of the electron in the molecular frame. Such experimental observation is well supported by a two-level quantum dynamics simulation including subcycle charge localization as well as a classical dynamics simulation incorporating a localized transient charge.

The measurements were performed in an ultrahigh vacuum chamber of cold target recoil ion momentum spectroscopy (COLTRIMS) [24,25], as schematically illustrated in Fig. 1. The elliptically polarized femtosecond laser pulse with a duration of 25 fs and a central wavelength of 790 nm was focused onto a supersonic molecular beam in the COLTRIMS. The three-dimensional momenta of the detected ionic fragments were retrieved from the measured time of flights and positions of the impacts. The peak

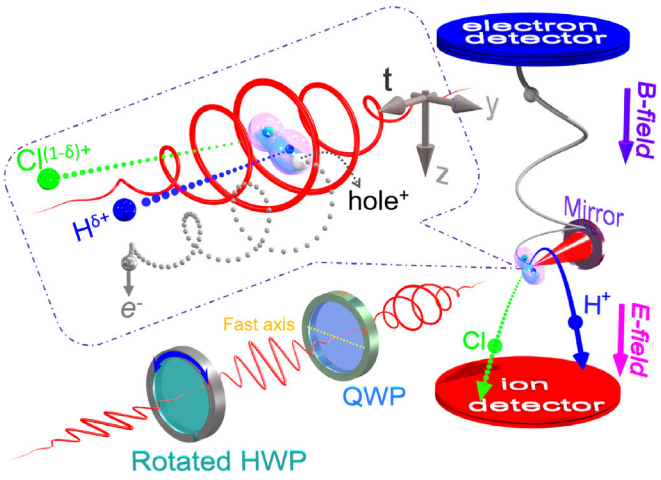

FIG. 1. Schematic diagram of the experimental setup. The LEP or REP (left- or right-handed elliptical polarization) laser fields with the same ellipticity and intensity are produced by rotating a half-wave plate (HWP) in front of a quarter-wave plate (QWP) with major axis along the y axis. The inset shows schematic traces of the outgoing nuclear fragments and the freed electron. The created hole$^+$, represented by a white ball, is shared by two outgoing nuclear fragments, whose charges evolve as $H^{\delta+}$ and $Cl^{(1-\delta)+}$ with time ($0 \le \delta \le 1$).

intensity and ellipticity of the laser field were estimated to be $I \sim 3.0 \times 10^{14}$ W/cm^2 and $\varepsilon \sim 0.72$, with its major and minor polarization axes along y and z, respectively, leading to tunneling ionization. Switching the helicity of the incident laser pulse with a motorized half-wave plate before a quarter-wave plate every two minutes ensured identical experimental conditions for the LEP and REP (left- or right-handed elliptical polarization) laser fields, which excludes any systematic error from the measurement and allows us to cross-check the results.

Driven by an elliptically polarized light, the tunneled photoelectron acquires a final momentum approximately perpendicular to the instantaneous electric field vector at the ionization instant according to the general principle of angular streaking [26–29]. As illustrated in the inset of Fig. 1, driven by a LEP laser field, a photoelectron (represented by a gray ball) freed by an instantaneous electric field pointing to $-y$ will primarily tunnel from the $+y$ site [30], and end up with a final momentum almost along the $+z$ axis. Meanwhile, H^+ emission direction gives the orientation of the molecule at the ionization instant according to the axial recoil approximation [31]. Thereby, by measuring the ejected photoelectron and the H^+ fragments in coincidence, the molecular orientation and the tunneling site of photoelectron in the molecular frame can be determined.

Figure 2(a) displays the measured momentum distributions of the H^+ fragments of the dissociative single ionization of HCl, i.e., $HCl \rightarrow H^+ + Cl + e^-$, which is denoted as the HCl(1, 0) channel, in the y-z plane driven by a LEP laser field. The concentrated distribution along the y axis indicates that the HCl molecule is favored to be ionized when the molecular bond is aligned along the major polarization axis (y axis) of the elliptically polarized laser field [32–34], and thus the final momentum of the released electron is mainly along the minor polarization axis (z axis). The radial momentum along the y axis mainly originates from the bond breakup. Conversely, driven by an optically symmetric multicycle laser pulse, any shift or asymmetry in the momentum distribution along the z axis is

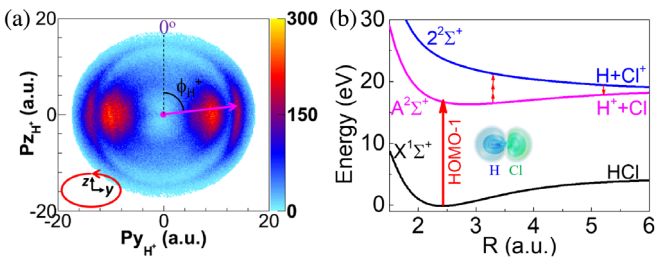

FIG. 2. (a) The measured momentum distribution of the H^+ fragments in y-z plane for the HCl(1, 0) channel induced by the LEP laser fields. ϕ_{H^+} is the emission angle of H^+ with respect to the $+z$ axis. (b) Relevant potential energy curves of HCl and HCl^+ (adapted from [23]) and the HOMO-1 orbital of HCl as the inset.

a signature of the Coulomb interaction from the released electron and the accumulated laser impulse, where the information of transient charge localization is embedded according to Eq. (1). We find that the laser impulse plays a dominant role, while the interaction from the released electron is less important [35]. Therefore, in the following, we focus on the impulse gained from the laser field. The amount of laser impulse (or transient ionic charge) can be quantified by analyzing the angular distribution of H^+ in the y-z plane, i.e., ϕ_{H^+} as illustrated in Fig. 2(a). The deviation of ϕ_{H^+} from $\pm 90°$ is a manifestation of the laser impulse accumulated by the H^+ fragments in the z direction. The direction of the major polarization axis of the laser field along the y axis is carefully calibrated by examining the angular distribution of the ejected protons in the dissociative double ionization of H_2 molecules with the same experimental conditions, in which no asymmetry is expected with respect to $\phi_{H^+} = \pm 90°$.

Two distinct rings are observed in the momentum map of the HCl(1, 0) channel in Fig. 2(a). We note that the H^+ fragments originating from the dissociative single ionization of H_2 in the background have almost the same momentum and thus overlap with that of the inner ring of the HCl(1, 0) channel [23], while the outer momentum ring is about 14 a.u. and has no overlap with the H^+ fragments from the H_2 molecule. Therefore, only the outer momentum ring is selected in the following analysis to unambiguously represent the HCl(1, 0) channel. As illustrated in Fig. 2(b), the outer momentum ring is most likely produced in the following pathway: by removing one HOMO-1 electron, a nuclear wave packet is created on the bound $A^2\Sigma^+$ state of HCl^+. It afterwards couples to the repulsive $2^2\Sigma^+$ state and then gets back to the $A^2\Sigma^+$ state via net two-photon processes and dissociates into H^+ and Cl fragments with a final momentum around 14 a.u. each.

Figure 3 shows the measured (open circles) angular distributions of the ejected H^+ fragments from the HCl(1, 0) channel driven by a LEP laser field when the correlated photoelectron ends up with a final momentum along $+z$ (blue case) or $-z$ (orange case) as illustrated in the inset sketches. Taking the orange case as an example, the photoelectron carrying a final momentum along $-z$ is released from the $-y$ site by the laser electric field when it points to $+y$. The measured H^+ fragments with ϕ_{H^+} around $-90°$ ($-y$ axis) or $+90°$ ($+y$ axis) stands for the cases where the electron is released with the tunneling exit near the H or Cl site, respectively, depending on the orientation of the HCl molecule. Two features can be observed in Fig. 3 for the orange case. On the one hand, the yield is higher around $\phi_{H^+} = -90°$ than that around $\phi_{H^+} = +90°$, indicating that the electron is preferentially released by laser fields pointing from H to Cl, which is dominated by the molecular orbital shape [23,32]. On the other hand, and more interestingly, the angular distribution is asymmetric with respect to the emission direction of $\phi_{H^+} = -90°$. Relative

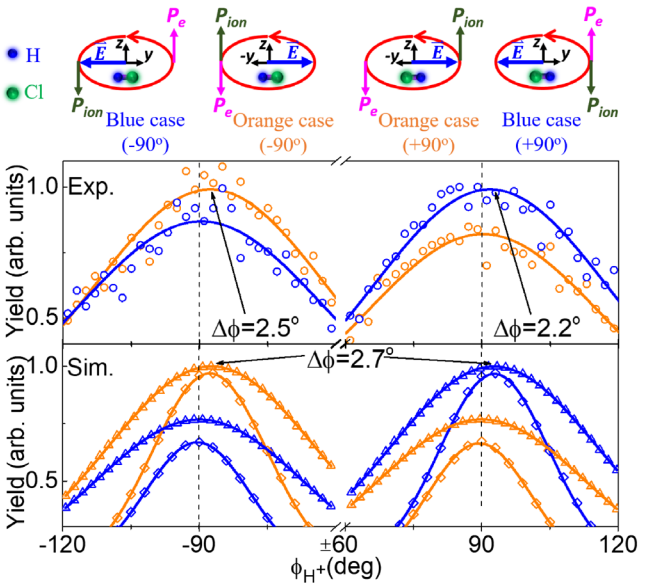

FIG. 3. The open circles (fitted with solid curves) are the measured angular distributions of the H^+ fragments of the HCl(1, 0) channel when the electron is released from two different sites driven by the LEP field as illustrated in the individual sketches. The vertical black dashed lines represent the positions of $\pm 90°$. $\Delta\phi$ is the offset angle of the peak position of the fitted curves with respect to the y axis ($\pm 90°$). The open triangles and diamonds (fitted with solid curves) are the corresponding classical and quantum simulation results, respectively.

to the black dashed line located at $\pm 90°$ (along the y axis), the peak position of the ϕ_{H^+} distribution is clearly right shifted with respect to the $-y$ axis ($\phi_{H^+} = -90°$), while it is almost symmetrically aligned with the $+y$ axis ($\phi_{H^+} = +90°$). This asymmetry indicates that the acquisition of laser impulse by the ejected H^+ is more efficient when the photoelectron is released with a tunneling exit near the H site of HCl. According to Eq. (1), the accumulated laser impulse is largely determined by the distribution of the ionic charge during the fragmentation process, thereby we conclude that there is a fraction of the positive charge that is transiently localized at the H side when the electron tunnels out with an exit near the H site of HCl; while almost no positive charge is transiently localized around H as the electron tunnels out with an exit near Cl.

Likewise, as displayed in Fig. 3, the laser impulse acquired by the H^+ fragments shows the similar electron tunneling site dependence for the blue case, in which the angular distribution is right shifted around $\phi_{H^+} = +90°$ as compared to the symmetric distribution around $\phi_{H^+} = -90°$. These features are also well reproduced when the helicity of elliptically polarized laser pulses is switched to REP [35]. We perform Gaussian fits (solid lines) to the measured data in Fig. 3 and obtain the most probable emission direction of ϕ_{H^+m}. In our experiment, the momentum accumulated by the photoelectron in the z direction is estimated to be around 0.8 a.u. and the momentum of the

H^+ fragments along the y axis is about 14 a.u., therefore the rotating angle of H^+ with respect to $\phi_{H^+} = \pm 90°$ should be less than 3.3°. The measured average offset angle of H^+ with respect to $\phi_{H^+} = \pm 90°$ is $\Delta\phi = ||\phi_{H^+m}| - 90°| = (2.4 \pm 0.3)°$ when the photoelectron is released with the tunneling exit near the H site of HCl, indicating approximately $(72 \pm 9)\%$ of the impulse is acquired by the H^+ fragments. If the impulse to HCl^+ was to deposit on its center of mass, the H^+ fragments would only acquire a share of $1/36$, much less than 72% observed in our experiment. This underlines the important role of the transient valence charge localization in determining the impulse partitioning among the nuclei of a breaking molecule.

To support our experimental findings, we carry out a two-level quantum dynamics simulation [35] where the fragmentation of the nuclear wave packet occurs on the $A^2\Sigma^+$ and $2^2\Sigma^+$ states. In order to simulate the rotation of the fragments, we employ a two-dimensional model including both stretching and rotation of the molecule. In this two-level model, asymmetric charge distribution is enabled by different populations on the $A^2\Sigma^+$ and $2^2\Sigma^+$ states on the subcycle level [35]. For a heteronuclear diatomic molecule, it is not surprising, from a symmetry point of view, to find asymmetric transient charge localization at the subcycle level. The heteronuclear nature of the molecule also leads to the asymmetric shape of the molecular orbital as well as results in a permanent dipole moment. For the extremely asymmetric molecule of HeH^+ [42–44], the strong permanent dipole results in the direct vibrational excitation, fundamentally different from that seen in homonuclear molecules, as the dominant fragmentation mechanism. For less asymmetric molecules such as HCl and CO [32,45], the effect of the molecular orbital shape often outweighs their permanent dipoles in inducing different populations on the $A^2\Sigma^+$ and $2^2\Sigma^+$ states, which is the case in our experiment [35]. Needless to say, the molecular orbital shape, or the molecular structure factor for tunneling ionization, varies within the laser pulse [14], its time dependence, however, only leads to an overall increase in the yield and hardly has any effect on the rotation angle of the H^+ fragment, and thus is neglected in our simulations [35]. The results of the quantum simulation are shown in Fig. 3 as open diamonds and fitted with solid curves, which reproduces our experimental observations.

In order to have a clear physical picture of how the asymmetric ejection of H^+ occurs, we carry out an additional classical dynamics simulation of the fragmentation process incorporating a transient charge on the respective fragments. The details of the numerical model can be found in the Supplementary Material [35]. Briefly, we employ two modes of charge localization in the optical field [35,43], one of which is transiently induced by the optical field on the subcycle level and the other is statically allocated to the composite H-Cl molecular ion. The results

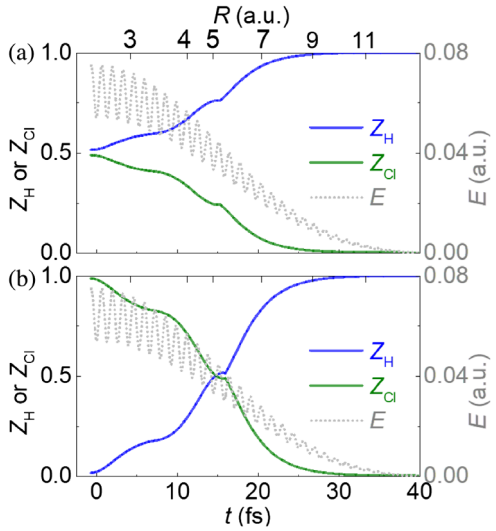

FIG. 4. (a) The evolution of the ionic charges of Z_H (blue curve) on the H and Z_{Cl} (green curve) on the Cl nuclei over time t and the internuclear separation R when the electron tunnels from the H site of HCl. The gray curve shows the magnitude of the laser electric field E. Tunneling occurs at $-T/4$ with T the laser period and $t = 0$ corresponding to the pulse center. (b) Same as (a) but for the case when the electron tunnels from the Cl site of HCl.

of the classical dynamics simulation, averaged over molecular orientation in the laser polarization plane, are shown in Fig. 3 as open triangles fitted with solid curves. The simulation clearly supports the experimental observation of an asymmetric angular distribution of the ejected H^+ depending on the electron tunneling site. When the electron tunnels out with an exit near H [Fig. 4(a)], an initial optical-field-induced transient charge, or electron hole generated by tunneling ionization, which is subject to subsequent rearrangements, is localized at H. Such transient concentration of positive charge on H leads to a substantial accumulation of laser impulse for H^+, resulting in an offset angle of 2.7°, close to the experimental value of about 2.4°.

On the other hand, when the electron tunnels out from the Cl side [Fig. 4(b)], the optical-field-induced transient charge is initially localized on Cl. The other static charge is given to the composite H—Cl, leaving almost no initial positive charge on H. Although the positive charge would move to the H side as the dissociation process goes on, substantial concentration of positive charge on H only occurs at the trailing edge of the laser pulse where the field strength is low, leading to minimal laser impulse in this case. Such minimal initial positive charge on H results in an almost symmetric angular distribution of the H^+ fragments around $\pm 90°$.

The above analysis can be clearly rationalized from Fig. 4, which shows the evolution of ionic charges on the nuclei over time t and internuclear separation R when the electron tunnels out near the pulse center at the H site

[Fig. 4(a)] or at the Cl site [Fig. 4(b)] of HCl. The magnitude of the laser electric field is shown in the same figure. The H fragment has a substantial positive charge when the laser field is on if the electron tunnels near the H site while it has minimal ionic charge if it is the other way round. The laser impulse accumulated by the electron in the z direction can be estimated easily with the help of Eq. (1), which, when divided by the momentum in the y direction from molecular breakup, gives roughly the rotation angle. With this simple physical picture, the H^+ rotation angles are estimated to be 1.95° and 0.05° when the electron tunnels from the H and Cl side, respectively, which are very close to our experimental values and simulation results. Therefore, it is the initial transient charge localization, when the laser field is on, that plays a crucial role in inducing the resulting rotation of the ionic fragments.

In summary, we have studied the tunneling-site-dependent laser impulse accumulated by the H^+ fragments in the strong-field dissociative single ionization of HCl by using an elliptically polarized femtosecond laser pulse. An asymmetry in the asymptotic momentum picked up by H^+ is found depending on the electron tunneling site in the molecular frame, which can be traced back to root from a transient valence charge localization induced by ultrafast strong-field tunneling ionization of molecules. When the electron tunnels out with an exit near H which digs a transient electron hole on this site, a positive transient charge is localized on H, leading to a much larger laser impulse to the H^+ fragments as compared to the mass-dominated scenario. A two-level quantum dynamics simulation and a classical dynamics simulation incorporating a transient charge localization support our experimental observations. Our work reveals the crucial role of the transient valence charge localization in strong-field tunneling ionization of molecules and will stimulate extensive investigations of tunneling-site-sensitive correlated electron-nuclear motion in a wide range of molecules.

This work is supported by the National Key R&D Program of China (Grants No. 2018YFA0306303 and No. 2018YFA0404802); the National Natural Science Foundation of China (Grants No. 11834004, No. 11904103, No. 11925405, and No. 91850203); the Science and Technology Commission of Shanghai Municipality (Grants No. 19JC1412200, No. 21ZR1420100); the 111 project of China (Grant No. B12024); and the Innovation Program of Shanghai Municipal Education Commission (2017-01-07-00-02-E00034). O. F. acknowledges the support of the ERDF Operational Program—Burgundy 2014/2020 and the EIPHI Graduate School (Contract No. "ANR-17-EURE-0002"). H. N. acknowledges helpful discussions with Yang Guo, Kunlong Liu, and Lun Yue. Numerical simulations were in part performed on the ECNU Multifunctional Platform for Innovation (001).

*hcni@lps.ecnu.edu.cn
†jwu@phy.ecnu.edu.cn

[1] L. Young *et al.*, Nature (London) **466**, 56 (2010).
[2] N. Rohringer, D. Ryan, R. A. London, M. Purvis, F. Albert, J. Dunn, J. D. Bozek, C. Bostedt, A. Graf, R. Hill, S. P. Hau-Riege, and J. Rocca, Nature (London) **481**, 488 (2012).
[3] M. S. Schoffler *et al.*, Science **320**, 920 (2008).
[4] A. Perry-Sassmannshausen, T. Buhr, A. Borovik, Jr., M. Martins, S. Reinwardt, S. Ricz, S. O. Stock, F. Trinter, A. Müller, S. Fritzsche, and S. Schippers, Phys. Rev. Lett. **124**, 083203 (2020).
[5] D. Rolles, M.s Braune, S. Cvejanović, O. Geßner, R. Hentges, S. Korica, B. Langer, T. Lischke, G. Prümper, A. Reinköster, J. Viefhaus, B. Zimmermann, V. McKoy, and U. Becker, Nature (London) **437**, 711 (2005).
[6] M. Drescher, M. Hentschel, R. Kienberger, M. Uiberacker, V. Yakovlev, A. Scrinzi, T. Westerwalbesloh, U. Kleineberg, U. Heinzmann, and F. Krausz, Nature (London) **419**, 803 (2002).
[7] E. Goulielmakis, Z.-H. Loh, A. Wirth, R. Santra, N. Rohringer, V. S. Yakovlev, S. Zherebtsov, T. Pfeifer, A. M. Azzeer, M. F. Kling, S. R. Leone, and F. Krausz, Nature (London) **466**, 739 (2010).
[8] H. Sann, C. Schober, A. Mhamdi, F. Trinter, C. Müller, S. K. Semenov, M. Stener, M. Waitz, T. Bauer, R. Wallauer, C. Goihl, J. Titze, F. Afaneh and L. Ph. H. Schmidt, M. Kunitski, H. Schmidt-Böcking, Ph. V. Demekhin, N. A. Cherepkov, M. S. Schöffler, T. Jahnke, and R. Dörner, Phys. Rev. Lett. **117**, 263001 (2016).
[9] J. P. Cryan, J. M. Glownia, J. Andreasson, A. Belkacem, N. Berrah *et al.*, Phys. Rev. Lett. **105**, 083004 (2010).
[10] L. Fang, M. Hoener, O. Gessner, F. Tarantelli, S. T. Pratt, O. Kornilov, C. Buth, M. Gühr, E. P. Kanter, C. Bostedt, J. D. Bozek, P. H. Bucksbaum, M. Chen, R. Coffee, J. Cryan, M. Glownia, E. Kukk, S. R. Leone, and N. Berrah, Phys. Rev. Lett. **105**, 083005 (2010).
[11] G. Kastirke, M. S. Schöffler, M. Weller, J. Rist, R. Boll *et al.*, Phys. Rev. Lett. **125**, 163201 (2020).
[12] G. Goldsztejn, T. Marchenko, R. Püttner, L. Journel, R. Guillemin, S. Carniato, P. Selles, O. Travnikova, D. Céolin, A. F. Lago, R. Feifel, P. Lablanquie, M. N. Piancastelli, F. Penent, and M. Simon, Phys. Rev. Lett. **117**, 133001 (2016).
[13] A. N. Markevitch, D. A. Romanov, S. M. Smith, and R. J. Levis, Phys. Rev. Lett. **92**, 063001 (2004).
[14] P. M. Kraus, O. I. Tolstikhin, D. Baykusheva, A. Rupenyan, J. Schneider, C. Z. Bisgaard, T. Morishita, F. Jensen, L. B. Madsen, and H. J. Worner, Nat. Commun. **6**, 7039 (2015).
[15] D. Jia, J. Manz, and Y. Yang, J. Chem. Phys. **151**, 244306 (2019).
[16] F. He, A. Becker, and U. Thumm, Phys. Rev. Lett. **101**, 213002 (2008).
[17] N. Takemoto and A. Becker, Phys. Rev. Lett. **105**, 203004 (2010).
[18] N. Takemoto and A. Becker, Phys. Rev. A **84**, 023401 (2011).
[19] V. Hanus, S. Kangaparambil, S. Larimian, M. Dorner-Kirchner, X. Xie, M. S. Schöffler, G. G. Paulus, A. Baltuška, A. Staudte, and M. Kitzler-Zeiler, Phys. Rev. Lett. **124**, 103201 (2020).

[20] M. Odenweller, N. Takemoto, A. Vredenborg, K. Cole, K. Pahl, J. Titze, L. P. H. Schmidt, T. Jahnke, R. Dörner, and A. Becker, Phys. Rev. Lett. **107**, 143004 (2011).
[21] M.-X. Wang, S.-G. Chen, H. Liang, and L.-Y. Peng, Chin. Phys. B **29**, 013302 (2020).
[22] J. Maurer and U. Keller, J. Phys. B **54**, 094001 (2021).
[23] H. Akagi, T. Otobe, A. Staudte, A. Shiner, F. Turner, R. Dörner, D. M. Villeneuve, and P. B. Corkum, Science **325**, 1364 (2009).
[24] J. Ulrich, R. Moshammer, A. Dorn, R. Dörner, L. Ph. H. Schmidt, and H. Schmidt-Böcking, Rep. Prog. Phys. **66**, 1463 (2003).
[25] R. Dörner, V. Mergel, O. Jagutzki, L. Spielberger, J. Ullrich, R. Moshammer, and H. Schmidt-Böcking, Phys. Rep. **330**, 95 (2000).
[26] P. Eckle, A. N. Pfeiffer, C. Cirelli, A. Staudte, R. Dörner, H. G. Muller, M. Büttiker, and U. Keller, Science **322**, 1525 (2008).
[27] A. N. Pfeiffer, C. Cirelli, M. Smolarski, R. Dörner, and U. Keller, Nat. Phys. **7**, 428 (2011).
[28] J. Wu, M. Meckel, L. Ph. H. Schmidt, M. Kunitski, S. Voss, H. Sann, H. Kim, T. Jahnke, A. Czasch, and R. Dörner, Nat. Commun. **3**, 1113 (2012).
[29] C. Hofmann, A. Bray, W. Koch, H. Ni, and N. I. Shvetsov-Shilovski, Eur. Phys. J. D **75**, 208 (2021).
[30] C. Huang, P. Lan, Y. Zhou, Q. Zhang, K. Liu, and P. Lu, Phys. Rev. A **90**, 043420 (2014).
[31] L. D. A. Siebbeles, M. Glass-Maujean, O. S. Vasyutinskii, J. A. Beswick, and O. Roncero, J. Chem. Phys. **100**, 3610 (1994).
[32] J. Ma, H. Li, K. Lin, Q. Song, Q. Ji, W. Zhang, H. X. Li, F. Sun, J. Qiang, P. Lu, X. Gong, H. Zeng, and J. Wu, Phys. Rev. A **97**, 063407 (2018).
[33] H. Li, X. M. Tong, N. Schirmel, G. Urbasch, K. J. Betsch, S. Zherebtsov, F. Süßmann, A. Kessel, S. A. Trushin, G. G. Paulus, K.-M. Weitzel, and M. F. Kling, J. Phys. B **49**, 015601 (2016).
[34] I. Znakovskaya, P. von den Hoff, N. Schirmel, G. Urbasch, S. Zherebtsov, B. Bergues, R. de Vivie-Riedle, K.-M. Weitzel, and M. F. Kling, Phys. Chem. Chem. Phys. **13**, 8653 (2011).
[35] See Supplemental Material at http://link.aps.org/supplemental/10.1103/PhysRevLett.127.183201 for more details, which includes Refs. [36–41].
[36] L. Xu and F. He, Chin. Sci. Bull. **65**, 4188 (2020).
[37] X.-M. Tong, Z. X. Zhao, and C. D. Lin, Phys. Rev. A **66**, 033402 (2002).
[38] S. F. Zhao, C. Jin, A.-T. Le, T. F. Jiang, and C. D. Lin, Phys. Rev. A **81**, 033423 (2010).
[39] O. I. Tolstikhin, T. Morishita, and L. B. Madsen, Phys. Rev. A **84**, 053423 (2011).
[40] Q. Sun, T. C. Berkelbach, N. S. Blunt, G. H. Booth, S. Guo, Z. Li, J. Liu, J. McClain, E. R. Sayfutyarova, S. Sharma, S. Wouters, and G. K.-L. Chan, WIREs Comput. Mol. Sci. **8**, e1340 (2018).
[41] G. Maroulis, Mol. Phys. **74**, 131 (1991).
[42] P. Wustelt, F. Oppermann, L. Yue, M. Möller, T. Stöhlker, M. Lein, S. Gräfe, G. G. Paulus, and A. M. Sayler, Phys. Rev. Lett. **121**, 073203 (2018).
[43] L. Yue, P. Wustelt, A. M. Sayler, F. Oppermann, M. Lein, G. G. Paulus, and S. Gräfe, Phys. Rev. A **98**, 043418 (2018).
[44] E. Dehghanian, A. D. Bandrauk, and G. Lagmago Kamta, J. Chem. Phys. **139**, 084315 (2013).
[45] J. Wu, L. Ph. H. Schmidt, M. Kunitski, M. Meckel, S. Voss, H. Sann, H. Kim, T. Jahnke, A. Czasch, and R. Dörner, Phys. Rev. Lett. **108**, 183001 (2012).